Magma compressibility and the missing source for some dike intrusions

Eleonora Rivalta[1,2] and Paul Segall[3]

Received 14 November 2007; revised 23 January 2008; accepted 30 January 2008; published 28 February 2008.

[1] Dike intrusions are often accompanied by localized deflation, interpreted as depressurizing magma chambers feeding the dike. In some cases the inferred volume decrease is a factor of 4 or 5 less than the volume increase of the dike. Here we explore whether this discrepancy can be explained by compressibility of the magma combined with the fact that cracks are much more compliant than equidimensional magma chambers. If pressure changes are small, the magma compressibility β_m is constant, and the dike ends up in hydrostatic equilibrium with an ellipsoidal magma chamber at the same depth, the ratio r_V of the volume of the crack to the volume lost by the chamber is $r_V = 1 + 4\mu\beta_m/3 > 1$, where μ is the host rock rigidity. For gas poor magmas, $\beta_m = 0.6–2 \cdot 10^{-10}$ Pa^{-1} and $\mu = 3–25$ GPa, we find $1.2 < r_V < 7.7$. Large changes in magma compressibility due to gas exsolution increase r_V.
Citation: Rivalta, E., and P. Segall (2008), Magma compressibility and the missing source for some dike intrusions, *Geophys. Res. Lett.*, *35*, L04306, doi:10.1029/2007GL032521.

1. Introduction

[2] The injection of dikes and sills is often accompanied by deflation of one or more magma reservoirs. In some cases the volume decrease of these reservoirs estimated from surface deformation data is too small to account for the increase in crack volume. For example, the 1997 dike intrusion into Kilauea's east rift zone was apparently fed both from summit and rift zone magma reservoirs as well as drainage of the Pu'u O'o magma pond [*Owen et al.*, 2000; *Segall et al.*, 2001]. The volume of the dike ($23 \cdot 10^6$ m^3), less volume provided by collapse of the Pu'u O'o lava pond ($12.7 \cdot 10^6$ m^3 [*Thornber et al.*, 2003]) is a factor of $\sim$3.8 greater than the inferred volume decrease in the two magma chambers (summit, $1.5 \cdot 10^6$ m^3, and Makaopuhi crater, $1.2 \cdot 10^6$ m^3 [*Owen et al.*, 2000]). Similarly, the 2005 dike intrusion in Afar was modeled by *Wright et al.* [2006] to have a volume of 2.5 km^3, while the associated deflation of two reservoirs at the northern end of the dike indicates a volume decrease of only 0.5 km^3. The trade-off between volume change and depth of the magma chambers results in an uncertainty in the inferred volume change of about 20% (T. Wright, personal communication, 2007), so that the volume ratio is $r_V = 5 \pm 1$.

[3] These results can be explained by invoking magma sources sufficiently deep that the surface deformation they produce is below measurement errors – a hypothesis difficult to falsify. Elastic layering (both inversions assumed homogeneous half-spaces) could bias the magma chamber depths and hence volume decreases, although it seems unlikely that this could explain the discrepancy. An alternative explanation is that exsolving volatiles increase the compressibility of the magma diminishing the pressure drop in the magma reservoirs [*Johnson*, 1992; *Johnson et al.*, 2000; *Huppert and Woods*, 2002; *Mastin et al.*, 2008].

[4] Clearly, mass is conserved, not volume. A full analysis must account not only for the compressibility of the melt, but of the magma chamber and the dike or sill. Magma chambers that can be modeled as ellipsoids are relatively stiff, whereas cracks (dikes and sills) are highly compliant. We show that these shape effects, together with magma compressibility, can explain volume ratios r_V substantially greater than one. A simple analogy may be filling balloons from a helium tank. The balloons are much more compliant than the steel tank, and the gas is highly compressible. Thus, many balloons can be filled with negligible change in volume of the tank.

[5] Gas exsolution strongly influences magma compressibility. Magma is, in general, a mixture of melt, crystals and volatiles, the latter partly dissolved in the liquid and partly in the gas phase. As magma ascends, volatiles exsolve forming bubbles leading to important changes in density and compressibility of the mixture.

[6] We consider a system composed of a magma chamber, representing the magma source, and a dike or sill, representing the magma sink, embedded in a homogeneous elastic half-space. Only the magma chamber is present in the initial state (Figure 1). In the final state the source is deflated and a magma-filled sink (sill or dike) is emplaced. First, we derive results for a simple geometry, with an ellipsoidal magma chamber feeding a horizontal sill at the same depth. Then, we extend our description to chamber and sill at different depths and finally to vertical dikes.

2. Physical Model

[7] We assume that magma extrusion from the chamber is slow enough that all chemical processes are in equilibrium, and that the chamber is recharged at an even slower rate from below, so that recharge does not contribute significantly to volume change during the intrusion. The amount of recharge depends in part on the time of the post-intrusion geodetic surveys. We also assume that all properties are uniform within the source and (separately) the sink, although we later allow properties to vary with depth in the dike. Consider an initial state (1) of the system with a

[1]Department of Physics, University of Bologna, Bologna, Italy.
[2]Now at School of Earth and Environment, University of Leeds, Leeds, UK.
[3]Department of Geophysics, Stanford University, Stanford, California, USA.

0094-8276/08/2007GL032521$05.00

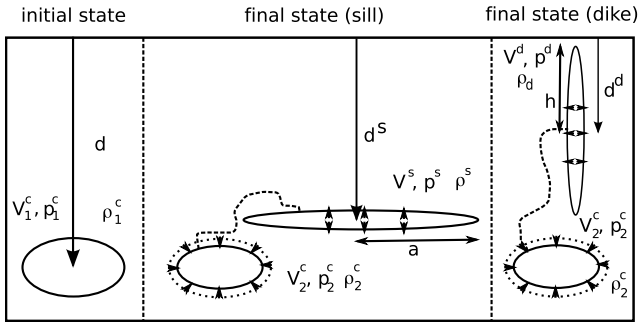

Figure 1. Sketch of the model: (left) in the initial state, an ellipsoidal magma chamber is buried at depth d. In the final state, (middle) a penny-shaped sill of radius a, or (right) an ellipsoidal dike with vertical semiaxis h, lateral semiaxis a and opening Δu, has formed at depth d^s or d^d respectively drawing melt from the chamber. The sill, or the dike, is connected to the chamber, so that the magma is in hydrostatic equilibrium in the final state.

magma chamber at depth d. In the final state (2) the chamber is decompressed by mass outflow from the chamber to a sink at depth d^s. Mass conservation requires:

$$\rho^c_1 V^c_1 = \rho^c_2 V^c_2 + \rho^s_2 V^s_2 \tag{1}$$

where ρ and V are density and volume respectively. Superscripts c and s refer to chamber and sink and subscripts 1 and 2 indicate initial and final state.

[8] We assume the process to be isothermal, so for a given initial volatile content, all variables depend solely on pressure p. If the chamber can be modeled as a pressurized ellipsoid, the elastic rock response to a pressure change can be described by a chamber compressibility:

$$\beta_c = (1/V)dV/dp = 3/(4\mu) \tag{2}$$

where μ is the shear modulus of host rock [*McTigue*, 1987; *Tiampo et al.*, 2000]. For small pressure variations we linearize the volume change as $V^c{}_2 = V^c{}_1[1 + \beta_c(p^c{}_2 - p^c{}_1)]$.

[9] The volume of a penny-shaped crack of radius a is

$$V^s = 8(1-\nu)a^3(p-\sigma)/3\mu = ba^3(p-\sigma) \tag{3}$$

where σ is the far-field crack normal-stress [*Sneddon*, 1951] and $b = 8(1-\nu)/3\mu$. Thus, the compressibility of the sink is $\beta_s = (1/V)\ dV/dp|_a = 1/(p-\sigma)$. Since typically the shear modulus is much greater than the magma over-pressure, $\beta_c \ll \beta_s$.

2.1. Constant Compressibility, Chamber and Sink at Same Depth

[10] We examine first the case $d^s = d$, such that hydrostatic equilibrium requires that the final pressure in the sink and chamber be the same: $p^c{}_2 = p^s{}_2 \equiv p_2$. Density in the initial and final state are functions of $p^c{}_1 \equiv p_1$ and p_2 respectively: $\rho^c{}_1 = \rho(p_1)$, $\rho^c{}_2 = \rho^s{}_2 = \rho(p_2)$. Mass conservation becomes:

$$\rho(p_1) = \rho(p_2)\left[1 + \beta_c(p_2 - p_1) + V^s_2/V^c_1\right] \tag{4}$$

[11] For magma with compressibility β_m, assumed constant over the pressure interval $[p_2, p_1]$, the density varies as

$$\rho(p_2) = \rho(p_1)[1 + \beta_m(p_2 - p_1)] \tag{5}$$

where we assume small pressure changes and $\beta_m = 1/\rho_m\, d\rho_m/dp$.

[12] Substituting (5) into (4) and neglecting second order terms the ratio:

$$r_V = -\frac{V^s_2}{V^c_2 - V^c_1} = -\frac{V^s_2}{V^c_1\beta_c(p_2 - p_1)} \tag{6}$$

can be obtained explicitly:

$$r_V = 1 + \frac{\beta_m}{\beta_c} = 1 + \frac{4\mu\beta_m}{3} \tag{7}$$

[13] Thus, the ratio r_V is equal to 1 only if the magma is incompressible or if the host medium is very compliant, $\beta_c \gg \beta_m$. Typically, rigidity in volcanic areas ranges from about 0.1 GPa for very fractured and compliant rocks to about 30 GPa or more for very stiff ones [*Gudmundsson*, 2005; *Dzurisin*, 2007, p. 281]. Compressibility of degassed basalts at crustal depths is in the range $0.4{-}2 \cdot 10^{-10}$ Pa^{-1} [*Spera*, 2000]. Thus, for degassed magma $1.05 < r_V < 9$. Negligible volume discrepancies may be expected for very degassed magmas intruding into extremely compliant crust. However, r_V significantly greater than one may be observed. Appropriate values for Kilauea volcano are $\beta_m = 0.6{-}1 \cdot 10^{-10}$ Pa^{-1} and $\mu = 3{-}25$ GPa [*Johnson*, 1992; *Johnson et al.*, 2000], giving for a gas-poor melt $r_V = 1.24{-}4.33$.

[14] Equation (7), which assumes constant magma compressibility, is valid as long as the pressure is far from saturation. Including effects of gas exsolution increases the ratio r_V, as discussed below.

2.2. Variable Compressibility, Chamber and Sink at Same Depth

[15] If a gas phase is present in the magma, we couple mass conservation with an equation of state $\rho_m(p)$. Ignoring crystals, the magma density is

$$\frac{1}{\rho_m} = \frac{V_g + V_l}{M_m} = \frac{V_g}{M_g}\frac{M_g}{M_m} + \frac{V_l}{M_l}\frac{M_l}{M_m} = \frac{\chi_g}{\rho_g} + \frac{1-\chi_g}{\rho_l} \tag{8}$$

where m, g and l refer to magma mixture, gas and liquid respectively, M is mass and $\chi_g = M_g/M_m$ is the mass fraction of the gas phase in the magma.

[16] We adopt two different approaches to model gas exsolution. Henry's law gives analytical expressions for a single volatile phase:

$$\chi_g = \chi_0 - sp^n \quad \text{if} \qquad \chi_0 - sp^n > 0 \tag{9}$$

and 0 otherwise where χ_0 is the total mass fraction of volatiles, dissolved or exsolved, s and n are constants for different volatile species and different magma types [*Sparks*, 1978, and references therein]. Equation (9) produces a non-realistic discontinuity in density and compressibility at saturation pressure. For multiple volatile

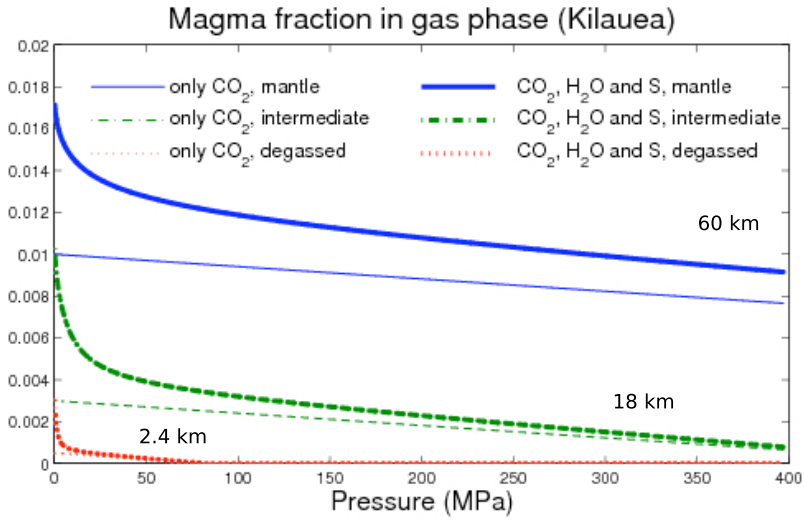

Figure 2. Mass fraction in gas phase for Henry's law (thin lines) and Mastin/Gerlach numerical exsolution model (thick lines). Different line styles correspond to different total volatile content appropriate for tholeiitic magma: 'mantle' indicates a gas-rich magma ($\chi(CO_2)$ = 1 wt%, $\chi(H_20)$ = 0.5 wt%), 'intermediate' refers to magma stored in a chamber ($\chi(CO_2)$ = 0.3 wt%, $\chi(H_20)$ = 0.4 wt%), and 'degassed' indicates volatile content as measured in Kilauea lava lakes ($\chi(CO_2)$ = 0.04 wt%, $\chi(H_20)$ = 0.27 wt%) (data from *Schmincke* [2004] and *Wallace and Anderson* [2000]). Approximate saturation depth for the three volatile concentrations is also indicated.

species we employ the algorithm of *Gerlach* [1986] and *Mastin* [1995] considering CO_2, H_2O and sulfur. Figure 2 compares the analytical and numerical approaches. We do not account for gas loss from the magma, hence gas content in the mixture may be overestimated at shallow depths.

[17] The density of the liquid phase is to first order $\rho_l(p) = \rho_0(1 + \beta_l p)$. We assume that gas behavior is described by the Ideal Gas Law: $\rho_g = M_{mol}\, p/RT$, where M_{mol} is the gas molar mass, R the gas constant and T the absolute temperature. Non-ideality of the gas phase is important for pressures larger than a few tens of MPa. We neglect this when considering shallow reservoirs and dikes. For deeper sources non-ideal gas behavior should be considered [see, e.g., *Holloway*, 1977].

[18] Mass conservation becomes:

$$\rho_m(p_1) = \rho_m(p_2)\left[1 + \beta_c(p_2 - p_1) + ba^3(p_2 - \sigma)/V_1^c\right] \qquad (10)$$

where, assuming Henry's law, magma density is

$$\rho_m(p) = \left[\frac{(\chi_0 - sp^n)RT}{M_{mol}p} + \frac{1 - \chi_0 + sp^n}{\rho_0(1 + \beta_l p)}\right]^{-1} \qquad (11)$$

for $\chi_0 - sp^n > 0$, and equal to $\rho_0(1 + \beta_l p)$ otherwise. Equation (10) is a transcendental equation for p_2 given p_1, and parameters, β_c, σ, and ba^3/V_1^c.

2.3. Chamber and Sink at Different Depths

[19] If d^s and d are different, mass conservation (10) provides one equation for two unknowns $p^c{}_2$ and $p^s{}_2$. The system of equations is closed by requiring hydrostatic equilibrium in the final state:

$$\int_{p_2^c}^{p_2^s} [\rho_m(p)]^{-1}\, dp = \int_d^{d^s} g\, dz \qquad (12)$$

Integrating,

$$F(p_2^c) - F(p_2^s) = g(d - d^s) \qquad (13)$$

where $F(p)$ is the primitive of the reciprocal of the magma density. With Henry's law the integral in (13) can be done analytically. Together, mass conservation and (13) provide a pair of coupled non-linear equations which can be solved for p_2^c and p_2^s given d and d^s, p_1, a, and V_1^c.

[20] Parameter values are listed in Table 1. Results for $d^s = d$ are illustrated in Table 2 and Figure 3 (solid line).

Table 1. Properties of Magma and Elastic Medium[a]

Property	Symbol	Range	Value
Basaltic Magma: Liquid Phase			
Density at p = 1 atm	ρ_0		2650 kg · m^{-3}
Compressibility	β_l	0.4–2 · 10^{-10}Pa^{-1}	1 · 10^{-10}Pa^{-1}
Basaltic Magma: Gas Phase			
Temperature	T		1450 K
Solubility (CO_2)	s		5.9 · 10^{-12}Pa^{-1}
Henry's law exponent	n		1
Solubility (H_2O)	s		6.8 · 10^{-8}Pa$^{-0.7}$
Henry's law exponent	n		0.7
Volatile mass fraction	χ_0	see Figure 2	see Figure 2
Elastic Medium			
Elastic rigidity	μ	3–20 GPa	20 GPa
Poisson's ratio	ν		0.25
Rock density	ρ_r		2700 kg · m^{-3}
Normal stress	σ		0.7ρ_r g z
Magma Sources			
Chamber radius	r_c	0.5–4 km	3 km
Chamber depth	d	4–10 km	5 km
Sink radius	a	1–10 km	5 km
Sink depth	d^s	2–10 km	5 km

[a]Parameters were varied over the range in column 3. If not otherwise specified, illustrations and results are given for values in column 4.

Table 2. Analytical (Henry) and Numerical (Gerlach) Values of r_V for Different Total Volatile Contents, $d = d^s = 5$ km

$\chi_0^{CO_2}$, wt%	$\chi_0^{H_2O}$, wt%	r_V (Henry)	r_V (Gerlach)
0.04	0.27	3.67	3.67
0.3	0.4	7.1	8.8
1	0.5	14.7	20.2

Table 3. Same as in Table 2 but for $d = 10$ km, $d^s = 5$ km

$\chi_0^{CO_2}$, wt%	$\chi_0^{H_2O}$, wt%	r_V (Henry)	r_V (Gerlach)
0.04	0.27	3.72	3.72
0.3	0.4	4.5	4.8
1	0.5	6.7	7.9

Numerical calculations show that for differences in saturation depth of up to a few tens of km, corresponding to differences in total volatile content of up to one order of magnitude, both the pressure drop at the magma chamber and the magma density change by a few percent. The mass lost from the chamber during dike injection is very small (less than 0.5% in our numerical models), however the ratio of dike volume to chamber volume decrease can be quite large (Table 2 and Figure 3). Equation (7) reproduces numerical estimates of r_V within 5%, except when $d = d_s$ = saturation depth, where discrepancies can be as much as 10% (Figure 3).

[21] Increasing the depth of the source reservoir diminishes the effect of gas exsolution on r_V, since volatiles remain dissolved in the magma (Figures 2 and 3 and Table 3). Nevertheless, as long as an appropriate compressibility is used, equation (7) represents a reasonable approximation (error less than 5%, Figure 3). Increasing the size of the magma chamber decreases r_V.

2.4. Vertical Dike

[22] For a vertical dike, a depth-dependent magma density can be included in the analysis. Mass conservation becomes:

$$\rho(p_1^c)V_1^c = \rho(p_2^c)V_2^c + \frac{\pi}{2}a\int_{-h}^{h}\Delta u[p(z)]\rho[p(z)]\,dz \qquad (14)$$

where we assumed an elliptical horizontal cross-section for the dike with a the half-length, h the half-height and Δu the dike opening. $\Delta u(z)$ is computed from the dike overpressure $p(z) - \sigma$, where $p(z)$ is found by requiring hydrostatic equilibrium with the magma chamber and within the dike itself. For this purpose, the displacement discontinuity method [*Crouch and Starfield*, 1983] can be used or the crack problem can be solved semianalytically for any prescribed overpressure as a series expansion in Chebyshev polynomials [*Bonafede and Rivalta*, 1999]. Computations show that r_V for a vertical dike is 3 to 7% less than for a sill of similar volume located at its mid point depth.

3. Results and Discussion

[23] Mass conservation applied to dike or sill intrusions fed by magma chambers shows that volumes in general are not conserved. Expected volume discrepancies depend mainly on stiffness of the host rock, shape of the sources involved, magma compressibility (affected by exsolving volatiles), depth of the sources and external stress field. For small changes in pressure, and an ellipsoidal magma chamber at the same depth as the crack, $r_V = 1 + 4\mu\beta_m/3$. The effect of gas exsolution is to increase r_V as it increases the compressibility of the magma. Gas loss has the opposite effect. We neglected the influence of layering, partly for consistency with the inversions at Kilauea and Afar, partly

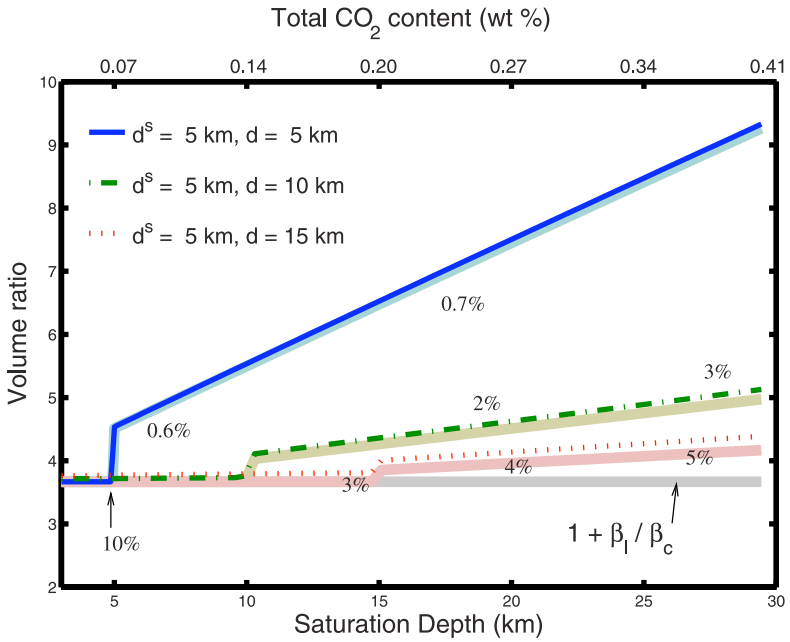

Figure 3. Volume ratio r_V as a function of total CO_2 content or its saturation depth. Thick bright lines show r_V as calculated from equation (7); percent discrepancies relative to the numerical results are annotated close to the relevant regions. Exsolution from Henry's law (9), for other parameters see Table 1.

in order to limit the analysis to first order effects. It is worth noting that only rigidity of rock around the magma chamber plays a role in equation (7). The rigidity of rock around the sill cancels out when neglecting second order terms. However, it would enter indirectly equation (14) for the dike opening displacement.

[24] We apply our results to geodetic inversions performed for the 1997 intrusion/eruption at Kilauea volcano, Hawaii [*Owen et al.*, 2000; *Segall et al.*, 2001], and the 2005 Afar intrusion [*Wright et al.*, 2006]. Using $\mu = 20$ GPa and $\beta_l = 1 \cdot 10^{-10}$ Pa^{-1} for Kilauea, the modelled lower bound value $r_V = 3.7$ is slightly smaller than the observed value $r_V^{obs} = 3.8 \pm 0.8$. This would be consistent with efficient degassing during storage in the summit magma chamber and vapor release during rifting. If a rigidity of 3 GPa and an unsaturated magma compressibility of $0.7 \cdot 10^{-10}$ Pa^{-1} are more appropriate, then $r_V = 1.3$, indicating a larger role played by exsolved gas during intrusion. Dike intrusion in Afar shows a greater volume discrepancy ($r_V = 5 \pm 1$). Magma is in this case associated with mid-ocean ridge magmatism and is close to the tholeiitic composition typical of Kilauea, possibly with lower initial volatile content [*Barberi and Varet*, 1977; *Schmincke*, 2004]. The higher volume discrepancy could be explained by a higher rigidity of the host medium.

[25] We conclude that compressibility effects may explain a large fraction of the apparent volume discrepancies observed, and that hidden sources of magma may not be required. This, of course, does not prove that they don't exist.

[26] Future work could consider magma supplied from a partially molten mush, as well as the dynamical problem in which the size of the dike is determined dynamically (as in the work by *Segall et al.* [2001]) rather than imposed as it was in this work.

[27] **Acknowledgments.** E.R. gratefully acknowledges financial support from GNV (Project V3-6 "Etna") and from the University of Bologna (Program "Marcopolo"). P.S. acknowledges support from NSF grant EAR-0537920. Comments by Larry Mastin and Norman Sleep helped improve the manuscript. Two anonymous reviewers contributed with valuable suggestions.

References

Barberi, F., and J. Varet (1977), Volcanism of Afar: Small scale plate tectonics implications, *Geol. Soc. Am. Bull.*, *88*, 1251–1266.

Bonafede, M., and E. Rivalta (1999), On tensile cracks close to and across the interface between two welded elastic half-spaces, *Geophys. J. Int.*, *138*, 410–434.

Crouch, S. L., and A. M. Starfield (1983), *Boundary Element Methods in Solid Mechanics*, Allen and Unwin, Winchester, Mass.

Dzurisin, D. (2007), *Volcano Deformation*, Springer, Berlin.

Gerlach, T. M. (1986), Exsolution of H_2O, CO_2, and S during eruptive episodes at Kilauea volcano, Hawaii, *J. Geophys. Res.*, *91*, 12,177–12,185.

Gudmundsson, A. (2005), The effects of layering and local stresses in composite volcanoes on dyke emplacement and volcanic hazard, *Geoscience*, *337*, 1216–1222.

Holloway, J. R. (1977), Fugacity and activity of molecular species in supercritical fluids, in *Thermodynamics in Geology*, edited by D. Fraser, pp. 161–181, D. Reidel, Dordrecht, Netherlands.

Huppert, H., and A. W. Woods (2002), The role of volatiles in magma chamber dynamics, *Nature*, *420*, 493–495.

Johnson, D. J. (1992), Dynamics of magma storage in the summit reservoir of Kilauea Volcano, Hawaii, *J. Geophys. Res.*, *97*, 1807–1820.

Johnson, D. J., F. Sigmundsson, and P. T. Delaney (2000), Comment on "Volume of magma accumulation or withdrawal estimated from surface uplift or subsidence, with application to the 1960 collapse of Kilauea Volcano" by T. T. Delaney and D. F. McTigue, *Bull. Volcanol.*, *61*, 491–493.

Mastin, L. G. (1995), A numerical program for steady-state flow of Hawaiian gas mixtures through vertical erupting conduit, *U.S. Geol. Surv. Open File Rep., 95-756*. (Available at http://pubs.er.usgs.gov/usgspubs/ofr/ofr95756)

Mastin, L., E. Roeloffs, N. M. Beeler, and J. E. Quick (2008), Constraints on the size, overpressure, and volatile content of the Mount St. Helens magma system from geodetic and dome-growth measurements during the 2004–2006+ eruption, in *A Volcano Rekindled: The Renewed Eruption of Mount St. Helens, 2004–2006*, edited by W. E. S. D. R. Sherrod, and P. H. Stauffer, chap. 22, U.S. Gov. Print. Off., Washington, D. C., in press.

McTigue, D. F. (1987), Elastic stress and deformation near a finite spherical magma body: Resolution of the point source paradox, *J. Geophys. Res.*, *92*, 12,931–12,940.

Owen, S., P. Segall, M. Lisowski, A. Miklius, M. Murray, M. Bevis, and J. Foster (2000), January 30, 1997 eruptive event on Kilauea Volcano, Hawaii, as monitored by continuous GPS, *Geophys. Res. Lett.*, *27*, 2757–2760.

Schmincke, H.-U., (2004), *Volcanism*, Springer, Berlin.

Segall, P., P. Cervelli, S. Owen, M. Lisowski, and A. Miklius (2001), Constraints on dike propagation from continuous GPS measurements, *J. Geophys. Res.*, *106*, 19,301–19,318.

Sneddon, I. N. (1951), *Fourier Transform*, McGraw-Hill, New York.

Sparks, R. (1978), The dynamics of bubble formation and growth in magmas: A review and analysis, *J. Volcanol. Geotherm. Res.*, *3*, 1–37.

Spera, F. (2000), Physical properties of magma, in *Encyclopedia of Volcanoes*, edited by H. Sigurdsson, pp. 171–190, Academic, San Diego, Calif.

Thornber, C. R., C. Heliker, D. R. Sherrod, J. P. Kauahikaua, A. Miklius, P. G. Okubo, F. A. Trusdell, J. R. Budhan, W. I. Ridley, and G. P. Meeker (2003), Kilauea East Rift Zone magmatism: An episode 54 perspective, *J. Petrol.*, *44*, 1525–1559.

Tiampo, K. F., J. B. Rundle, J. Fernandez, and J. O. Langbein (2000), Spherical and ellipsoidal volcanic sources at Long Valley caldera, California, using a genetic algorithm inversion technique, *J. Volcanol. Geotherm. Res.*, *102*, 189–206.

Wallace, P., and A. T. Anderson (2000), Volatiles in magmas, in *Encyclopedia of Volcanoes*, edited by H. Sigurdsson, pp. 149–170, Academic, San Diego, Calif.

Wright, T. J., C. Ebinger, J. Biggs, A. Ayele, G. Yirgu, D. Keir, and A. Stork (2006), Magma-maintained rift segmentation at continental rupture in the 2005 Afar dyking episode, *Nature*, *442*, 291–294.

E. Rivalta, School of Earth and Environment, University of Leeds, Leeds LS2 9JT, UK. (e.rivalta@see.leeds.ac.uk)

P. Segall, Department of Geophysics, Stanford University, Mitchell Building, 397 Panama Mall, Stanford, CA 94305, USA. (segall@stanford.edu)